



Use of a heated graphite scrubber as a means of reducing interferences in UV-absorbance measurements of atmospheric ozone

Andrew A. Turnipseed, Peter C. Andersen, Craig J. Williford, Christine A. Ennis, and John W. Birks

2B Technologies, Inc., 2100 Central Ave., Boulder, CO 80301, USA

Correspondence to: Andrew A. Turnipseed (andrewt@twobtech.com)

Received: 4 January 2017 – Discussion started: 17 January 2017

Revised: 3 May 2017 – Accepted: 9 May 2017 – Published: 15 June 2017

Abstract. A new solid-phase scrubber for use in conventional ozone (O_3) photometers was investigated as a means of reducing interferences from other UV-absorbing species and water vapor. It was found that when heated to 100–130 °C, a tubular graphite scrubber efficiently removed up to 500 ppb ozone and ozone monitors using the heated graphite scrubber were found to be less susceptible to interferences from water vapor, mercury vapor, and aromatic volatile organic compounds (VOCs) compared to conventional metal oxide scrubbers. Ambient measurements from a graphite scrubber-equipped photometer and a co-located Federal equivalent method (FEM) ozone analyzer showed excellent agreement over 38 days of measurements and indicated no loss in the scrubber's ability to remove ozone when operated at 130 °C. The use of a heated graphite scrubber was found to reduce the interference from mercury vapor to $\leq 3\%$ of that obtained using a packed-bed Hopcalite scrubber. For a series of substituted aromatic compounds (ranging in volatility and absorption cross section at 253.7 nm), the graphite scrubber was observed to consistently exhibit reduced levels of interference, typically by factors of 2.5 to 20 less than with Hopcalite. Conventional solid-phase scrubbers also exhibited complex VOC adsorption and desorption characteristics that were dependent upon the relative humidity (RH), volatility of the VOC, and the available surface area of the scrubber. This complex behavior involving humidity is avoided by use of a heated graphite scrubber. These results suggest that heated graphite scrubbers could be substituted in most ozone photometers as a means of reducing interferences from other UV-absorbing species found in the atmosphere. This could be particularly important in ozone monitoring for compliance with the United States (U.S.) Clean Air Act or for use in

VOC-rich environments such as in smog chambers and monitoring indoor air quality.

1 Introduction

Ozone (O_3) in the lower atmosphere is produced by a complex set of photochemical reactions involving oxides of nitrogen and volatile organic compounds (VOCs). It is well established that anthropogenic emissions of these precursors lead to the production of elevated levels of ozone (Haagen-Smit and Fox, 1954; Chameides and Walker, 1973). It also is recognized that high levels of ozone are deleterious to human health (White et al., 1994; Weisel et al., 1995; Burnett et al., 1997; U.S.-EPA, 2016) and lead to plant and crop damage (Avnery et al., 2011; Emberson et al., 2003, 2009). For these reasons, the Clean Air Act in the United States (U.S.) and similar laws in other countries have set limits on ozone concentrations in ambient air. Enforcement of compliance with the U.S. National Ambient Air Quality Standards (NAAQS) requires monitoring of ozone concentrations at hundreds of locations, especially during summer months when photochemical ozone production is highest.

Currently, compliance monitoring of ozone is done almost exclusively by the method of UV absorbance at 253.7 nm due to the simplicity and reliability of this technique. However, it has been shown that UV photometers suffer from positive interferences from other trace gases that absorb at 253.7 nm such as mercury (Hg) and VOCs (Huntzicker and Johnson, 1979; Grosjean and Harrison, 1985; Kleindienst et al., 1993; Spicer et al., 2010). In addition, water vapor, which does not

absorb at 253.7 nm, is also a significant interference in commercial ozone analyzers (Meyer et al., 1991; Kleindienst et al., 1993) due to its ability to change the transmission of light through the absorbance cell (Wilson and Birks, 2006). Field observations have noted possible interferences in conventional UV-absorbance ozone monitors in very highly polluted areas, such as Houston, TX (Ollison et al., 2013), and Mexico City (Leston et al., 2005); however, other extensive studies have not shown evidence of biases, even near urban areas (Ryerson et al., 1998; Parrish and Fehsenfeld, 2000). Average concentrations of interfering species found in outdoor air would normally be expected to cause errors of only a few ppb at most, but this is well within measurement limits of UV ozone photometers when averaged over the 1 h time frame typical for compliance monitoring. Since high levels of interferences often coincide with high levels of ambient outdoor ozone (Leston et al., 2005; Ollison et al., 2013), a small, unpredictable bias would be difficult to discern and could result in regions being in noncompliance with the EPA ozone standard. The recent downward revision of the standard from 75 to 70 ppb (8 h average) is expected to increase the number of U.S. counties being out of compliance from 224 to 241 (McCarthy and Lattanzio, 2016), making small ppb-level interferences a more critical issue.

Other applications where interferences can play a significant role in biasing UV-absorption O₃ measurements include chamber-type experiments and the monitoring of indoor ozone. In the former, high VOC concentrations are typically used to enhance photochemistry (e.g., Leston et al., 2005; Griffin et al., 1999) or to generate aerosols (e.g., Lee et al., 2006), thus requiring accurate O₃ concentrations to be made in VOC-rich atmospheres. Indoor ozone concentrations are typically 20–80 % of that measured outdoors (U.S.-EPA, 2016); however, interfering species such as VOCs and mercury can be at much higher concentrations indoors from attached garages, cooking emissions, unvented heaters, the use of paints, cleaners, and outgassing from building components. This places even more stringent constraints on ozone monitors to reduce biases in these indoor environments.

Ambient ozone UV-absorbance measurements are conducted by observing the attenuation of transmission of the mercury emission line at 253.7 nm (near the maximum in the ozone absorption spectrum) through an absorbance cell. Relative light intensities are measured for a direct air sample (I) and an air sample where the ozone is removed by some type of ozone scrubber (I_0), and the ozone concentration is computed using the Beer–Lambert law. Ozone scrubbers are typically composed of manganese dioxide, charcoal, Hopcalite, metal-oxide-coated screens, or heated silver wool and play a key role in the degree to which interferences compromise the ozone readings in UV-absorption photometers. For chemical species that absorb 253.7 nm light, the degree of interference depends on the compound's absorption cross section, its ambient concentration, and the degree to which the compound is removed by the scrubber. If not removed

by the scrubber, its concentration remains constant between I and I_0 measurements and cancels out in the Beer–Lambert law. Thus the ideal scrubber would have two characteristics: (1) it would quantitatively remove ozone and (2) it would not remove other species that absorb at 253.7 nm or that otherwise modify light transmission to the detector such as water vapor. The metal oxide scrubbers used in conventional commercially available ozone photometers do not fully meet the second criterion, leading to errors in the Beer–Lambert law calculation of ozone.

A further, less obvious problem with UV-absorbing species is that they can desorb from the solid-phase scrubber at later times, causing a negative absorbance (value of I_0 is less than I in ozone-free air), thus imparting a negative bias to the overall measurement. This desorption can be caused by temperature or relative humidity (RH) changes within the scrubber that alter the adsorption characteristics of a species and allows it to be released back into the gas phase. Because UV-absorbing compounds and mercury are commonly present to some degree in both indoor and outdoor air, these interferences may be responsible in part for the baseline drift that occurs in photometric ozone monitors (Birks et al., 2013; Ollison et al., 2013). Therefore, development of a solid-phase scrubber that effectively destroys ozone ($\geq 99\%$ destruction) but efficiently passes interfering species is desirable.

Table 1 provides a list of several atmospheric constituents with known 253.7 nm absorption cross sections along with a selectivity ratio (S), defined as the ratio of the ozone cross section to that of the interfering compound at 253.7 nm. Notable among these are VOCs that contain an aromatic group. The absorption cross sections of these compounds vary widely, but can be similar to that of ozone, depending on the types of functional groups attached. Gaseous mercury is a particularly strong interference because the electronic energy levels of Hg atoms are resonant with the Hg emission line used in most ozone monitors. The relative response of mercury has been estimated at ~ 1 ppb O₃/ppt Hg (Spicer et al., 2010; Li et al., 2006). So even a few ppt of mercury vapor can potentially cause substantial biases in ozone measurements.

In this study we present a means of greatly reducing the interferences of mercury, UV-absorbing VOCs, and water vapor in ozone measurements by replacing conventional metal oxide internal ozone scrubbers with a heated graphite scrubber (Birks et al., 2016). Carbon-based scrubbers have often been used for removing ozone from air (Shields et al., 1999; Lee and Davidson, 1999). However, these scrubbers also effectively remove many other compounds (such as VOCs and water) by adsorption due to their large surface area (typically 500–3000 m² g⁻¹) and thus provide no significant advantage over existing ozone scrubbers. On the other hand, carbon in the form of graphite has a more ordered planar structure with less surface area (often < 20 m² g⁻¹) and fewer sites available for adsorption of possible interfering compounds. We show that a heated graphite scrubber composed of one or more graphite tubes effectively destroys ozone while effi-

Table 1. Properties of VOCs and other atmospheric species that are potential interferences in UV-absorption-based ozone measurements.

Interferent (INT)	Ambient mixing ratio ^a , ppb	σ_{254}^b , 10 ⁻¹⁷ cm ² molecule ⁻¹	e_v^c , (25 °C) mm Hg	S^d , ppb INT/ppb O ₃
Used in this study				
<i>p</i> -Xylene	0.3–30	0.057	8.84	20.2
Phenol	≤ 0.02	0.16	0.350	7.1
<i>p</i> -Tolualdehyde	< 1	0.55	0.250	2.09
<i>o</i> -Nitrophenol	≤ 0.001	2.15	0.113	0.53
Mercury	0.0002–0.003	1860 ^e	0.002	0.0005
Typical atmospheric constituents				
NO ₂	≤ 100	0.001	741	1000
SO ₂	1–25	0.014	3000	77
Methanol	≤ 40	< 0.00001	127	> 10 000
Acetone	0.2–9	0.0030	231	290
Formaldehyde	0.5–75	0.00029	3890	3960
Acetaldehyde	0.1–18	0.0015	902	590
1,3-Butadiene	0.1–6	< 0.02	1840	> 58
Trichloroethene	≤ 0.2	0.0041	69	265
2-Butanone	0.1–8	0.0031	90.6	370
Isoprene	0.1–5.5	0.0052	550	220
Octane	0.02–13	< 0.0002	14.1	> 5700
Methacrolein	0.02–1.7	0.00018	155	6400
Methyl vinyl ketone	0.2–1.5	0.00024	152	4790
Acetic acid	0.5–10	< 0.0006	15.7	> 1900
α -Pinene	≤ 0.4	0.00054	4.75	2120
d-Limonene	≤ 0.1	0.015	1.55	77
Aromatics				
Benzene	0.9–26	0.03	94.8	38
Toluene	0.05–39	0.039	28.4	29
<i>o</i> -Xylene	0.4–1	0.048	6.5	24
Ethylbenzene	0.08–16.5	0.052	9.6	22
Styrene (vinyl benzene)	0.06–3.1	1.3	6.4	0.88
1,3,5-Trimethylbenzene	0.03–4.2	0.037	2.48	31
<i>m</i> -Cresol	≤ 0.004	0.108	0.11	10.6
Benzaldehyde	0.1–1	0.09	0.127	12.8
Naphthalene	0.01–0.1	1.07	0.08	1.07
Nitrobenzene	0.02–0.40	1.3	0.245	0.88

^a Typical concentration ranges reported in Finlayson-Pitts and Pitts (2000), Seila et al. (1989), Mahmoud et al. (2002), Bernardo-Bricker et al. (1995), Delhomme et al. (2010), Davies (2003), Eiguren-Fernandez et al. (2004), Liu et al. (2002), Denis et al. (2006). ^b Absorbance cross sections at 253.7 nm taken from Keller-Rudek et al. (2013) and the related web database (<http://www.uv-vis-spectral-atlas-mainz.org/>). ^c Vapor pressures taken from <http://pubchem.ncbi.nlm.nih.gov/>. ^d Selectivity ratio, $S = \sigma_{O_3} / \sigma_{int}$, at 253.7 nm. To estimate the maximum response that a particular interferent could give in an ozone monitor, divide the ambient mixing ratio by the selectivity ratio, S . ^e From Birks et al. (2009).

ciently passing most UV-absorbing species and is relatively insensitive to humidity changes. Our results suggest that replacement of conventional scrubbers in commercially available ozone photometers with heated graphite scrubbers could increase their accuracy by reducing potential interferences.

2 Experimental

Most experiments were carried out with modified FEM 2B Technologies single-beam Model 202 and dual-beam Model 205 or Model 211 ozone monitors. Figure 1a shows a diagram of a typical single-beam UV ozone photometer such as the Model 202. Ambient air samples are drawn into the instrument through an inlet via an air pump. A solenoid valve alternately switches the gas sample directly into the optical detection cell or through an ozone scrubber and then

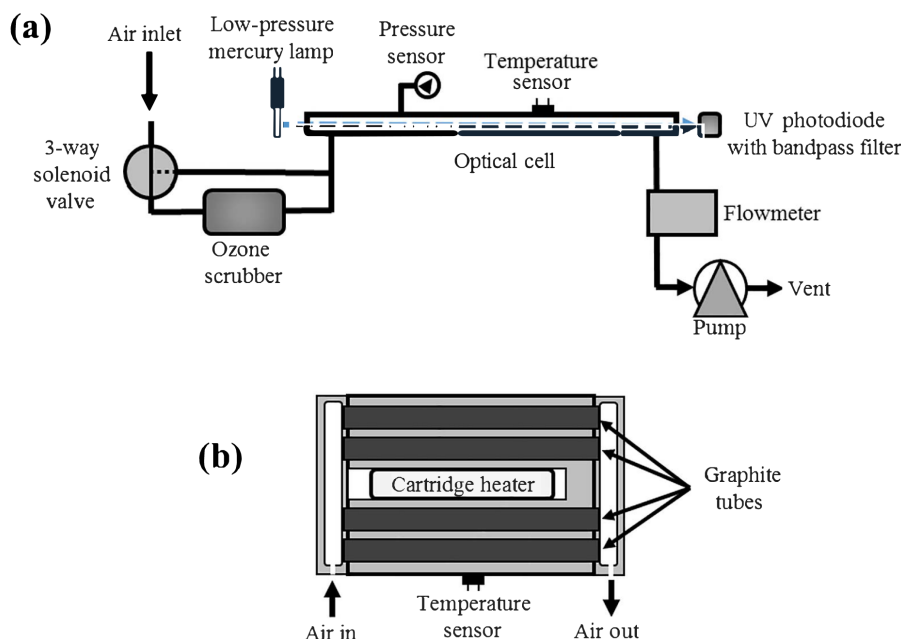


Figure 1. (a) Schematic diagram of a typical single-beam UV-absorbance monitor for ozone. (b) Schematic of the heated graphite scrubber consisting of four graphite tubes contained within a temperature-controlled aluminum block.

into the detection cell. UV light from a low-pressure mercury lamp passes through the detection cell and is detected by a photodiode containing a built-in interference filter centered at 254 nm. The ozone concentration is calculated using the Beer–Lambert law,

$$[\text{O}_3] = \frac{1}{\sigma L} \ln\left(\frac{I_0}{I}\right), \quad (1)$$

where σ is the absorption cross section for ozone ($1.15 \times 10^{-17} \text{ cm}^2 \text{ molecule}^{-1}$), L is the path of the detection cell, I_0 is the lamp intensity at the detector in the absence of ozone, and I is the lamp intensity with ozone present. The path length (L) is 15 cm for the 2B Technologies Model 202 and Model 205 ozone monitors. The Model 205 (and Model 211) analyzer differs in that it is a typical dual-beam instrument containing two optical cells irradiated by the same lamp, but with each cell equipped with its own photodiode. Two three-way solenoid valves are switched to alternate passage of ozone-scrubbed and un-scrubbed air through the two cells, providing a simultaneous measurement of I and I_0 . These analyzers were modified to locate the ozone scrubber outside of the instrument, allowing for easy exchange between the different scrubbers tested. Mixtures of interfering compounds in air were sampled into the ozone analyzers via an overflow tee where excess air was vented through a second scrubber to the atmosphere. All analyzers used were operating at manufacturer specifications.

Graphite scrubbers consisted of different combinations of graphite tubes (1/4 in o.d. and 1/8 in i.d., Ohio Carbon Blank, EDM-AF5 graphite) housed in a temperature-

controlled aluminum block. Tube lengths were either 7.6 cm (3 in) or 15.2 cm (6 in). Most results were obtained using four 7.6 cm tubes plumbed in parallel as shown in Fig. 1b. Using multiple tubes increased both surface area and residence time while still maintaining high flow conductance. This configuration was chosen because it quantitatively destroyed (>99 %) ozone in the single-beam Model 202 Ozone Monitor and fit within both Model 202 and 205 instruments. The aluminum block was heated with a cartridge heater (Thermal Corp., no. CPN20528), whose temperature could be varied up to 160 °C and controlled to within ± 2 °C. The graphite tubes were cleaned before use by heating at 300 °C for 12 h while purging with ultra-high purity (UHP) nitrogen and sonication for 20 min in dilute Micro-90 glass cleaner followed by rinsing with distilled water and drying. Scrubbers consisting of coarsely ground EDM-AF5 graphite ($\sim 1\text{--}3$ mm diameter particles) were also tested and exhibited similar properties for both ozone destruction and the reduction of interferences. However, we present results from the tube scrubbers because their geometric surface area and residence times were more easily characterized.

Other commercially available scrubbers were included in this study for comparison. These include the conventional packed-bed Hopcalite scrubber used in 2B Technologies analyzers as well as manganese-oxide-coated screens from a Thermo Electron Model 49C and a Teledyne Advanced Pollution Instrumentation (API) Model 400E. We also tested heated silver wool scrubbers similar to scrubbers used by Horiba. It should be noted that although these various scrubbers were used within 2B Technologies analyzers, pressure

and flow conditions were similar to those in the respective commercial analyzers. However, small differences in operating conditions of the various commercial analyzers may alter results in those instruments compared to those presented here.

Dry air (<2% relative humidity) was produced using a zero air generator (Aadco, Model 737) or from cylinders of zero grade air. Ozone-air mixtures and ozone-free air were produced via an ozone calibrator – a Model 306 Ozone Calibration Source™ (2B Technologies). The Model 306 instrument qualifies as an EPA transfer standard for ozone and can produce known mixing ratios of ozone via UV photolysis of air in the range between 0 and 1 ppm. Humidity was varied by humidifying the source air for the Model 306. A mixing tee was placed on the source line of the Model 306 with one end pulling through a water bubbler and the other through a drying tube (Drierite). Needle valves on each line allowed for independent control over the source line between the dry and humid air. Humidity was measured in the overflow just downstream of the ozone monitor via a temperature-humidity sensor (Omega, model HH311).

Mercury vapor was introduced to the ozone analyzer by using a glass diffusion tube. A small amount of liquid mercury was placed in a glass bulb, and vapor was allowed to diffuse through a 20 cm long capillary tube (i.d. = 0.5 mm). At the exit of the capillary tube, a small sweep flow of air (~5–15 cc min⁻¹) purged the mercury vapor into the main airflow (~3 L min⁻¹). Mercury concentrations were varied by immersing the reservoir and capillary tube in an insulated water bath and varying the temperature of the bath (0 to 60 °C). From bath temperature, flow rates, and the mercury vapor pressure, estimated mercury vapor concentrations of 0.3 to 30 ppb were produced. Mercury interference measurements were made relative to the 2B packed-bed Hopcalite scrubber.

Table 1 summarizes the absorption cross sections at 253.7 nm for a variety of atmospheric species including compounds tested in this study. Test compounds were chosen because they are either common outdoor (*p*-xylene) or indoor (phenol) pollutants or for comparison with previous studies (Spicer et al., 2010). Typically, gas mixtures between 5 and 25 ppm were made in preconditioned gas cylinders by dilution of the pure compound in UHP nitrogen. These were further diluted with zero grade air via mass flow controllers to produce mixing ratios in the range of 0.01–1.4 ppm. Low-volatility (*o*-nitrophenol) VOCs were added using diffusion tubes in a similar way to that described for mercury above. Sample purity was assessed using a gas chromatograph with flame ionization and mass spectrometric detection (GC-FID-MS). The VOC-air mixtures were sampled into ozone analyzers equipped with different scrubbers from an overflow tee. In some experiments, the VOC-air flow was simultaneously sampled into the inlet system of a gas chromatograph equipped with a flame ionization detector (GC-FID). VOC samples were pre-concentrated via a cooled (–5 °C) focusing trap containing Tenax TA (typically 100–500 cm³ of the

VOC-air mixture) and then rapidly heated to inject as described in Greenberg et al. (1994). Both GC systems were calibrated with a National Institute of Science and Technology certified primary standard of neohexane in nitrogen or a secondary VOC standard containing isoprene and camphene.

3 Results and discussions

As mentioned previously, any species absorbing light at 253.7 nm will be detected if its concentration is changed by the ozone scrubber, and thus an ideal ozone scrubber would remove all ozone but quantitatively pass interferences such as water vapor and UV-absorbing species. The following sections test the graphite scrubber against this ideal, followed by comparative tests with existing conventional scrubbers for known interferences.

3.1 Ozone removal efficiency

It has long been known that ozone reacts with graphite (Henning, 1965; Tracz et al., 2003), causing loss of the carbon surface (Razumovskii et al., 2007) with the assumed production of CO and CO₂. CO and CO₂ have been identified as the primary products from reactions of ozone with carbon black aerosols which are thought to be similar to graphitic carbon (Stephens et al., 1989; Smith and Chughtai, 1996; Saathoff et al., 1998). CO, CO₂, and other possible low-volatility hydrocarbons which could be lost to the gas phase tend to show negligible absorption at 253.7 nm (Table 1) compared to ozone. A graphite scrubber is not catalytic (i.e., there is actual loss of the scrubber carbon), but it can be estimated that a typical 7.6 cm long graphite tube would require a continuous 200 ppb ozone exposure at a flow rate of 1 L min⁻¹ for 213 days to lose 1% of its carbon; at 100 °C oxidation by ambient O₂ is also negligible (Entegris, 2015).

Initial tests of the graphite scrubber using four parallel 15.2 cm graphite tubes at room temperature showed nearly complete removal of ozone up to 250 ppb in the Model 202; however, the ozone removal efficiency degraded over several hours as the graphite surface became oxidized. Heating the graphite tubes to 100–130 °C resulted in complete recovery of the graphite's reactivity toward ozone, but large negative absorbances were observed in the ozone analyzers as the temperature of the graphite scrubber exceeded 145 °C. This was due to the emission of various volatile organic hydrocarbons from the graphite tubes as verified by GC-MS. We attribute this to either the thermal breakdown of the organic binder contained in graphite that is added during manufacturing or to initiation of O₂ oxidation, although the latter is not expected to be significant below about 350 °C (Entegris, 2015). Below 135 °C, emissions were greatly reduced and, after completing the cleaning process described above, typically resulted in a small negative offset (~–2 to –5 ppb) that remained constant over time. The exact cause of this

small residual negative offset is unclear, although it is likely due to residual organics that are slowly released from the hot graphite. As in the case of conventional ozone scrubbers, this small offset can be incorporated into the calibration parameters of the ozone analyzer.

We conclude that a tube configuration consisting of four 3.175 mm (1/8 in) i.d., 7.62 cm (3 in) long parallel graphite tubes (Fig. 1b), which easily fit within the existing Model 202 Ozone Monitor enclosure, provides adequate (>98 %) ozone destruction efficiency comparable with conventional scrubbers. This scrubber has an internal volume of 2.4 cm³ and a geometric surface area of 30.4 cm², resulting in a residence time of 0.145 s for a typical flow rate of 1 L min⁻¹. At a temperature of 100 °C and pressure of 1 atm, on average each ozone molecule collides with the surface 1.85×10^4 times while passing through the scrubber. Thus, assuming rapid diffusion to the walls, a collisional reaction probability γ of $\sim 1.7 \times 10^{-3}$ is required to assure >99 % ozone destruction. This is similar in magnitude to previously determined probabilities of ozone uptake on fresh carbon soot surfaces (Burkholder et al., 2015). The results discussed in the remainder of this paper were observed with this scrubber design, although the graphite surface area could be increased if necessary. Figure 2 shows examples of calibration plots where the ozone was varied and the graphite scrubber was alternately replaced with a conventional packed-bed Hopcalite scrubber. To test for reproducibility, four different sets of graphite tubes were used within the heater. Slopes of heated graphite vs. Hopcalite ozone measurements ranged from 0.96 to 1.01 among the different sets for concentrations up to 500 ppb of ozone. The overall average slope was 0.98. All calibration plots were highly linear with $R^2 > 0.99$, and their slopes were invariant over the graphite scrubber temperature range of 100–130 °C.

3.2 Long-term reliability of the graphite scrubber

A primary concern with carbon-based scrubbers is that as the surface of the solid-phase carbon oxidizes, it becomes less reactive toward ozone. In principle, the carbon is oxidized to CO and CO₂, which desorb to the gas phase and are swept away in the case of a flowing analyzer. However, the oxidation to CO and CO₂ in the presence of water vapor typically occurs in several steps through various oxygenated intermediates (i.e., epoxides, alcohols, aldehydes, and ketones), and it is likely that at least some of the carbon lost is in the form of small oxygenated organics such as formaldehyde, acetone, and acetaldehyde. These do not present a problem as long as they do not absorb appreciably at 253.7 nm. Ellis and Tometz (1972) were among the first to note that upon exposure to high ozone concentrations, coconut charcoal becomes less efficient at removing ozone as it oxidizes. This suggests that oxygenated hydrocarbons on the graphite surface or oxygen functionalities incorporated within the graphite structure have slower ozone reaction rates. A loss in reactivity toward

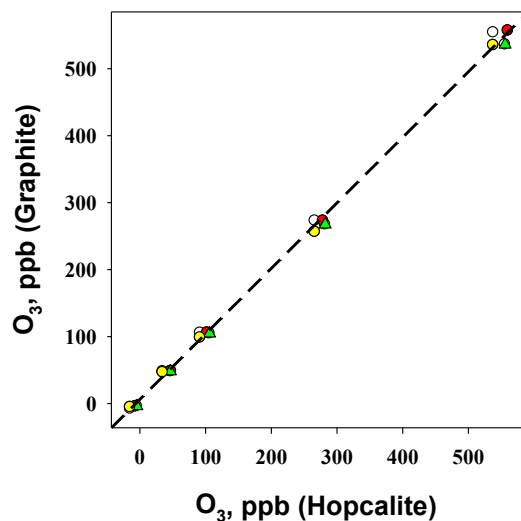


Figure 2. Plot of ozone measured with the graphite scrubber (at 100 °C) vs. that measured with the conventional Hopcalite scrubber. The different symbols/colors represent different sets of graphite tubes used within the heater during our reproducibility testing. Results were obtained using a 2B Technologies Model 202 single-beam ozone analyzer. The dashed line drawn is the 1 : 1 line.

ozone has also been observed for graphite at high (~ 0.5 %) levels of ozone (Razumovskii et al., 2007). We also observed this loss in ozone removal efficiency at room temperature and found that heating the graphite scrubber remedies this problem. At elevated temperatures (100 °C), continuous exposure of 150 ppb of ozone for 22 h in the single-beam Model 202 showed no loss of the graphite's ability to destroy ozone.

However, incorporation of the graphite scrubber into a dual-beam Model 205 led to unexpected complications. We found that even at 100 °C, it was necessary to reduce the flow rate to the minimum required to flush the absorbance cells in order to observe 100 % ozone removal. Furthermore, overnight exposure (18 h) of the graphite tubes to 150 ppb of O₃ in the dual-beam Model 205 resulted in a 10 % loss of the ozone removal efficiency. Exposure to higher ozone concentrations (300–700 ppb) in the dual-beam Model 205 resulted in faster temporal decays which leveled off at ~ 85 % ozone removal efficiency after 2 to 8 h. The graphite's capacity to destroy ozone could be restored by periodically heating the graphite to 150 °C for 20–30 min or by removal of the ozone exposure while continuing with normal analyzer operation for 3–6 h. Ellis and Tometz (1972) also had noted that removal of charcoal from ozone exposure for several hours resulted in a regeneration of the surface reactivity toward ozone.

These observations suggest a competition between ozone oxidizing the graphite surface (making less reactive species at the surface) and loss of these oxidized carbon-containing compounds to the gas phase (which presumably exposes new, less oxidized surface area). This competition helps explain

why the single-beam Model 202 is less susceptible to losing reactivity toward ozone since the scrubber is only exposed to ozone flow half of the time (during the I_0 measurement). During the I measurement, there is no flow through the scrubber, but oxidized compounds can still desorb and regenerate the surface. In the dual-beam monitor, the graphite is continuously exposed to a flow of ozone as it is always directed to one of the two cells for an I_0 measurement. As a result, the surface is being oxidized faster than the graphite can regenerate. One also expects this competition to be dependent upon the temperature of the scrubber and the flow rate through it as well as the ozone concentration.

Therefore, before the graphite scrubber can be used in long-term continuous monitoring, it is necessary to fully understand its limitations in terms of its loss of ozone removal efficiency. To further characterize the graphite scrubber, we undertook extended ambient ozone measurements on the 2B Technologies roof in Boulder, CO, during August and September of 2015. A single-beam Model 202 was equipped with our heated graphite scrubber (denoted as 202-G) and sampled from the same Teflon inlet line as an FEM (Federal equivalent method) Model 205 dual-beam analyzer with a conventional packed-bed Hopcalite scrubber (205-H). The Model 205 was equipped with Nafion for humidity equilibration; however, Nafion was removed from the Model 202 graphite scrubber analyzer (humidity interference is discussed in Sect. 3.3). Calibrations were performed on both instruments prior to and periodically throughout the comparison with a Model 306 ozone calibrator. Although the 205-H may be more susceptible to interfering compounds (described in following section), the anticipated bias is < 3 ppb.

We initially evaluated the graphite scrubber temperature at 100 °C since we had observed no loss of ozone removal efficiency during lab ozone exposure experiments with our single-beam ozone instrument. Ambient measurements were made from 8–24 August 2015. Ozone data was averaged to 5 min from both instruments (205-H and 202-G) and compared each day. The daily regression slopes were near unity (0.99 ± 0.02) for the first 12 days; however, on the 13th day, comparisons showed that the 202-G analyzer underestimated peak afternoon ambient ozone by $\sim 8\%$ and the 202-G continued to drop over the next 3 days, yielding a regression plot slope of ~ 0.85 versus the 205-H. This is shown in Fig. 3c, where the slopes of the daily comparison between the 202-G and 205-H are shown as a function of the cumulative ozone exposure (in ppm h). The calibration of the 202-G was rechecked and confirmed the scrubber only removed $86 \pm 2\%$ of the ozone passing through it.

The graphite was regenerated by heating to 150 °C for 1 h with no ozone present, and the calibration slope returned to 1.01 ± 0.02 . The 202-G was then returned to sampling, but the graphite scrubber was maintained at 130 °C – the highest temperature without inducing significant VOC emission from the graphite tubes as described in Sect. 3.1. Post-regeneration, the analyzers were compared again from

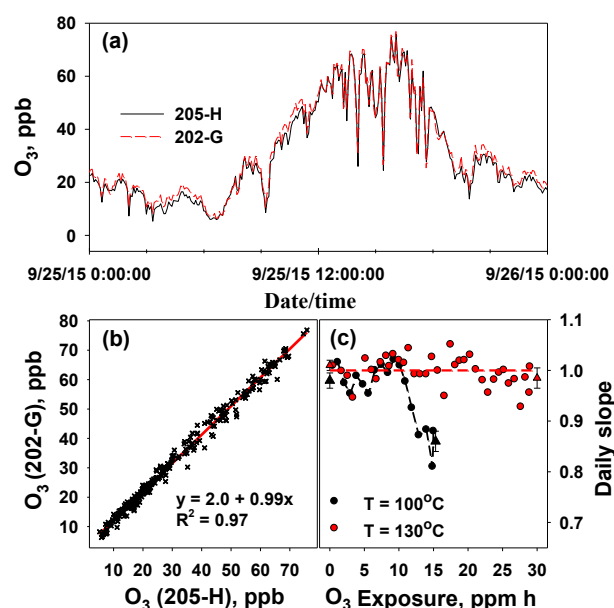


Figure 3. (a) Time series of 5 min averaged ozone concentrations measured in Boulder, CO, on 26 September 2015. (b) Correlation plot between the Model 202 (202-G, equipped with graphite scrubber) and the FEM Model 205 (205-H, Hopcalite scrubber and Nafion) for 26 September 2015. (c) Plot of the daily correlation plot slope vs. cumulative ozone exposure for the 202-G analyzer. Each point represents a single day. The graphite scrubber was initially maintained at 100 °C, regenerated, and then operated at 130 °C (see text for further explanation). Triangles represent calibration slopes pre- and post-intercomparison.

24 August to 30 September 2015 (38 days). Figure 3a shows a diurnal plot of the ozone measured by the two analyzers on 26 September 2015, near the end of the intercomparison. It is clear from this plot and the regression plot of the same data in Fig. 3b that there was excellent agreement between the two instruments. The daily intercomparison slope vs. ozone exposure in Fig. 3c confirms there was no graphite scrubber efficiency loss after 38 days (or 30 ppm h ozone exposure). A recheck of the analyzer calibrations found them to be within the uncertainty of the initial calibrations. Subsequent measurements using a dual-beam Model 211 equipped with a heated graphite scrubber operating at 130 °C indicate that there is also no loss in the ozone removal efficiency after exposure to 20 ppm h of ozone. Therefore, it appears the graphite scrubber must be maintained at temperatures greater than 100 °C for reliable long-term continuous monitoring. A temperature of 130 °C appears to be optimal for maintaining the balance between oxidation of the graphite by ozone and the loss of oxidized carbon from the surfaces to regenerate fresh carbon.

3.3 Interference testing

As mentioned earlier, carbon-based scrubbers (typically charcoal or activated carbon) remove ozone from air, but they also effectively remove many other species such as VOCs and water and thus would introduce interferences in ozone measurements. However, the more ordered planar structure of graphite and the greatly reduced surface area provide fewer sites for adsorption of interfering species. The results of our interference testing described below were performed with the graphite scrubber heated to 100 °C. Heating the graphite scrubber to 130 °C (the more optimal temperature found in our subsequent longevity testing described in the previous section) would likely reduce adsorption of water, mercury, and aromatic VOCs. Hence, these results can be viewed as a conservative estimate of the expected behavior of the graphite scrubber in reducing interferences in ozone measurements.

3.3.1 Water vapor

Previous studies have shown that rapid humidity changes can cause large apparent ozone absorptions (equivalent to tens of ppb) in most commercial ozone analyzers (Kleindeinst et al., 1993; Wilson and Birks, 2006; Spicer et al., 2010). Wilson and Birks (2006) explained this behavior as being due to changes in the refractive index at the surface of the optical cell resulting from varying amounts of water vapor adsorbed to cell walls. Initial experiments with a Model 202 analyzer equipped with a conventional Hopcalite scrubber, but no Nafion tube, indicated large signal changes coinciding with changes in humidity (Fig. 4, black dashed line). A large positive interference was observed as humidity was rapidly increased (uptake of water by the scrubber) and an opposite negative interference seen upon changing from humid to drier air (release of water from the scrubber). Figure 4 (magenta line) confirms that placement of a Nafion tube at the entrance to the optical cell to equilibrate the humidity with surrounding air (same humidity for I and I_0) effectively eliminates the water vapor interference, as shown earlier by Wilson and Birks (2006). A drawback of this approach is that Nafion tubing is expensive, and the length of tubing required to attain adequate equilibration can place limits on its use in miniaturized analyzers or can introduce flow restrictions, thus making it impractical in some applications.

The graphite scrubber proposed also mitigates artifacts caused by changing water vapor concentrations. As seen in Fig. 4, the initial large change in humidity does cause an apparent absorption of ~ 10 ppb of O₃ with the graphite scrubber in line. It appears that some water is initially taken up by the graphite, likely due to the somewhat porous nature of the graphite structure. However, water content within the graphite scrubber equilibrates within about 2 min and returns to its original value, whereas the Hopcalite trap remains compromised for > 15 min. Subsequent removal of the high wa-

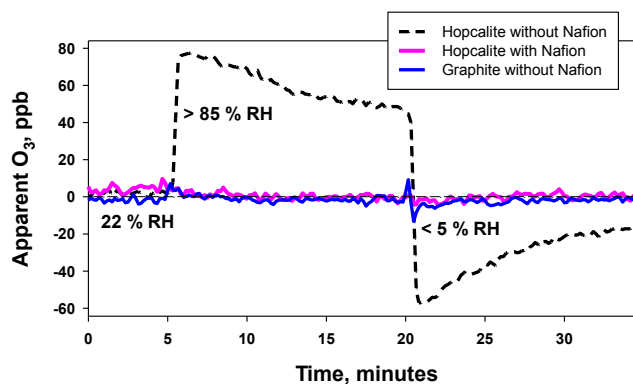


Figure 4. Time series showing the response of a Model 202 ozone analyzer to changes in relative humidity with no ozone present and different scrubbers.

ter vapor concentration leads to a negative response as water vapor desorbs from each scrubber. But again, the recovery of the graphite scrubber is relatively rapid compared to the Hopcalite, so although there is some water uptake, equilibration is rapid enough to exceed typical humidity changes and 30–60 min ozone averages will be relatively unaffected.

Variation of relative humidity did indicate a slight water dependency in the graphite scrubber and exhibited some differences between different graphite tubes. Figure 5 illustrates this behavior, showing two different sets of graphite tubes (four tubes in parallel, 7.6 cm long). Set #1 indicated about a +2.5 ppb change from dry to near-saturated air; whereas Set #2 was essentially independent of the humidity. Given graphite's hydrophobic nature, these differences are perplexing but could be due to differing degrees of oxidation on the graphite surface or on binders within the graphite, making the surface slightly more hydrophilic. The graphite scrubber's low sensitivity to humidity was also confirmed in our ambient measurements (Sect. 3.2), where we observed no correlation between ambient humidity changes and concentration differences between the graphite-equipped Model 202-G and the Hopcalite- and Nafion-equipped Model 205-H.

3.3.2 Mercury

Gaseous elemental mercury concentrations are typically less than a few ppt in ambient air, but mercury poses a problem in ozone photometers because typically the Hg atomic absorption line is used as the photometer's excitation source (Hg line at 253.7 nm). Birks et al. (2009) estimate that common ozone photometers could be 1860 times more sensitive to elemental mercury than ozone (Selectivity = 1.86 ppb O₃/ppt Hg) depending on how efficiently the scrubber removes mercury. Recent measurements in our laboratory showed that mercury absorbs ~ 1350 times more strongly than ozone in the Model 202 Ozone Monitor using the packed-bed Hopcalite scrubber (Birks, 2016, unpublished data). There is also evidence suggesting that the efficiency of

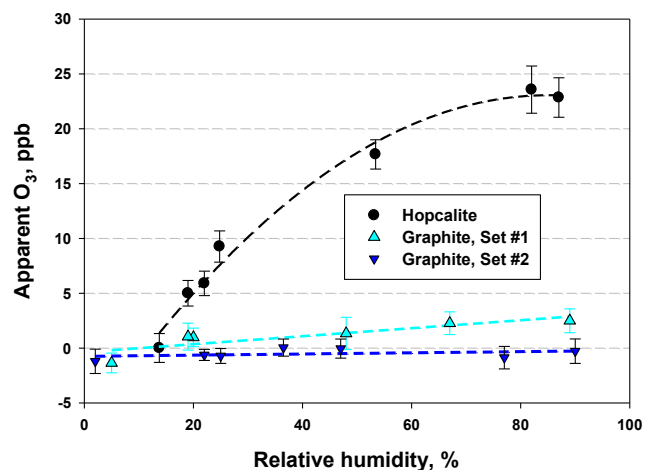


Figure 5. Humidity dependence of two different heated (100 °C) graphite scrubbers as well as that of a Hopcalite scrubber. The ozone analyzer was a 2B Technologies Model 202 single-beam instrument. Data points were 2 min averages obtained 15 min after a change in relative humidity. Error bars are 1σ of the 2 min average. The experiment was conducted at 20 °C. Note that the step changes in humidity were not as large as those shown in Fig. 4, thus leading to smaller observed artifact signals for the Hopcalite scrubber.

mercury uptake in several conventional scrubbers may depend on humidity (U.S.-EPA, 1999; Spicer et al., 2010), implying that these may act as a temporary reservoir capable of releasing mercury at later times following humidity changes.

In order to examine possible interferences due to elemental mercury, varying concentrations of mercury vapor were added to the Model 202 ozone monitor and responses were monitored (in apparent ppb of ozone) while the various graphite and conventional scrubbers were interchanged. As we did not have an independent measurement of mercury vapor concentrations, all measurements were made relative to the conventional packed-bed Hopcalite scrubber used in the 2B Technologies analyzers. For different levels of mercury additions, Fig. 6 shows the apparent ozone measured by the photometer as various scrubbers were alternated with the packed-bed Hopcalite. Five different sets of graphite tubes (a set is four tubes in parallel, each 7.6 cm long) were tested, and the slopes of plots of apparent ozone concentration vs. those obtained for the Hopcalite scrubber ranged from < 0.01 to 0.03 (median set is shown in Fig. 6). One set showed no measurable response to mercury up to an apparent ozone concentration of 2200 ppb for the Hopcalite scrubber. Noting above our recent observation that mercury absorption is 1350 times stronger than ozone (or 1.35 ppb O₃/ppt Hg), this leads to a response ratio of ≤ 0.04 ppb O₃/ppt Hg for the graphite scrubber. Measurements made at 22 and 80 % RH exhibited no differences (Fig. 6). In addition, measurements made with and without Nafion tubing inserted before the optical cell gave identical results, suggesting that mercury is neither lost nor interacts significantly with Nafion.

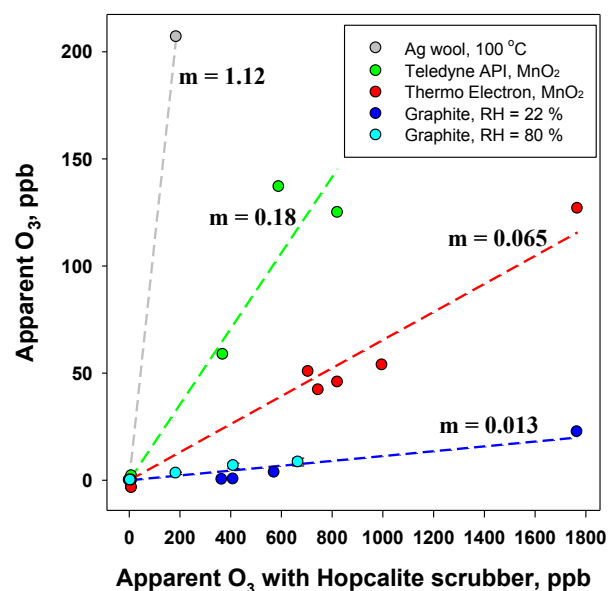


Figure 6. Apparent ozone measured in the Model 202 single-beam ozone analyzer using different ozone scrubbers, relative to the standard Hopcalite scrubber, upon addition of mercury vapor to ozone-free air. Slopes are given by the m values. The graphite scrubbers were heated to 100 °C for these tests.

The heated silver wool scrubber exhibited the largest mercury response, with a slope slightly greater than unity compared to Hopcalite (Fig. 6). Silver is known to rapidly form an amalgam with mercury (Dumarey et al., 1985), which likely explains this large response. Previous studies have shown that both the 2B Technologies Hopcalite scrubber and heated silver wool scrubber remove mercury vapor efficiently – reporting response ratios between 0.6 and 1.1 ppb O₃/ppt Hg (Spicer et al., 2010; U.S.-EPA, 1999). We report a response ratio of 1.49 ppb O₃/ppt Hg for the heated silver wool, assuming 1.35 ppb O₃/ppt Hg for the Hopcalite scrubber – approximately 1/3 higher than the previous studies. The sensitivity to Hg depends on the width of the emission line of the lamp (Birks et al., 2009), which may vary from instrument to instrument.

Both the Teledyne API and Thermo Electron scrubbers used screens coated with MnO₂ and showed less interference from mercury vapor compared to the packed-bed Hopcalite scrubber (slopes of 0.18 and 0.065). This yields response ratios of 0.24 and 0.09 ppb O₃/ppt Hg for the Teledyne API and Thermo Electron scrubbers, respectively. Smaller responses are likely due to the large reduction in scrubber surface area by use of the coated screens. Measurements made at both high (≥ 80 %) and low (20 %) relative humidity showed no significant differences, although the considerable scatter in the data likely obscures any small humidity dependencies. The interference of mercury in ozone photometers with MnO₂-based scrubbers has been the subject of several previous investigations. The U.S.-EPA (1999) reported response

ratios in the range of 0.12 to 0.24 ppb O₃/ppt Hg using a Thermo Electron scrubber. This study also suggested a lowering of the response ratio with increasing humidity. Higher response ratios (0.87 and 0.6 ppb O₃/ppt Hg) have also been reported in dry air (Li et al., 2006; Spicer et al., 2010). Spicer et al. (2010) also reported that the response ratio decreased by a factor of 2 when using humidified air (RH ~ 80 %), which is closer to both our results and those of the EPA. As will be shown for VOCs in the next section, it is likely that even a small amount of water vapor can cause a significant change in the adsorption properties of these solid-phase scrubbers; thus, the higher response ratios determined in dry air may not be applicable to sampling of ambient air. The use of a heated graphite scrubber can reduce the interference in ozone photometers from mercury vapor by a factor of ≥ 30 over the packed-bed Hopcalite scrubber and by a factor of ≥ 2 over the best solid-phase scrubber.

This low response ratio is only matched by using the gas-phase nitric oxide (NO) titration as a means of scrubbing ozone. In the recently introduced 2B Technologies Model 211 Scrubberless Ozone Monitor™, gas-phase NO titration eliminates the need for a solid-phase scrubber and effectively eliminates interferences from both UV-absorbing species and water vapor (Birks et al., 2013). However, a source gas of NO is required, reducing the portability of the instrument and adding long-term cost. The heated graphite scrubber avoids these disadvantages.

In general, mercury is not expected to be a significant interference in outdoor ambient air. Although there are some elevated measurements of mercury vapor in urban areas of Asia (up to ~ 3 ppt: Fang et al., 2004; Liu et al., 2002; Kim and Kim, 2002), concentrations typically range from 0.2 (background) to 0.5 (urban) ppt (Obriest et al., 2008; Weiss-Penzias et al., 2003; Denis et al., 2006). However, gas-phase mercury can reach higher levels near industrial or mining sources. Elevated mercury levels have also been shown to be present for indoor air (Carpi and Chen, 2001; Garetano et al., 2006). Because indoor ozone concentrations are typically low (~ 20–80 % of outdoor air, U.S. EPA, 2016), mercury poses a larger potential problem for indoor air quality monitoring of ozone. For example, Carpi and Chen (2001) report indoor mercury concentrations of up to 520 ng m⁻³ (~ 63 ppt). This would correspond to measured absorbances equivalent to ~ 85 ppb O₃ with the packed-bed Hopcalite, ~ 6–15 ppb O₃ with conventional MnO₂ screens, and < 2.6 ppb O₃ using the heated graphite.

3.3.3 Volatile organic compounds (VOCs)

Interferences from volatile organic compounds are more complicated due to the wide variety of compounds and their properties. There are many diverse atmospheric VOCs having a wide range of 253.7 nm absorption cross sections, volatilities, and potential responses to humidity. Along with the VOC absorption cross sections, Table 1 also lists room

temperature vapor pressures as an indicator of volatility. Aromatic VOCs are the most important when discussing interferences in ozone monitors, since the conjugation between the carbon–carbon double bonds both shifts the absorption spectrum to longer wavelengths and results in larger UV cross sections. Addition of various functional groups (hydroxyl, aldehyde, nitro, etc.) to the aromatic ring can further increase the absorption cross section. Furthermore, substitutions often result in lower volatility, making these species more likely to be retained in a solid-phase scrubber.

Interferences from VOCs typically result from two different mechanisms: (1) adsorption of the compound by the scrubber, resulting in a positive bias, and (2) subsequent later desorption of that compound from the scrubber due to eventual elution and/or changes in temperature or humidity that yield a negative bias. These two processes are complex functions of environmental conditions (temperature and humidity), volatility, and chemical properties of the specific VOC, as well as the reactivity and surface area of the scrubber material.

Past studies of VOC interferences have typically been of three types: (1) measurement of total net ozone biases during irradiation of simulated atmospheres in smog chambers (Kleindeist et al., 1993; Leston et al., 2005), (2) simultaneous atmospheric measurements by different analyzers using different measurement techniques (Ollison et al., 2013; Dunlea et al., 2006), and (3) addition of selected VOCs to ozone analyzers to determine the interference from that particular VOC (Grosjean and Harrison, 1985; Spicer et al., 2010). All of these approaches contribute to our understanding of the significance of VOC interferences in ozone monitors; however, we have chosen the latter approach to initially evaluate our heated graphite scrubber because it is a more direct approach and reproducible signals can be easily quantified. We chose *p*-xylene, phenol, *p*-tolualdehyde, and *o*-nitrophenol as test VOCs since they have reported 253.7 nm absorption cross sections ranging from 5×10^{-19} (*p*-xylene) to 2.15×10^{-17} (*o*-nitrophenol) cm² molecule⁻¹ (Keller-Rudek et al., 2013) and vapor pressures (25 °C) of 0.11 to 8.8 mm Hg.

VOC interferences in dry air

Initial experiments examined VOC interferences in dry air (RH < 3 %) in the absence of ozone using a single-beam Model 202 monitor equipped with the various scrubbers described above. No Nafion tubing was installed upstream of the optical cell in the monitor. VOC concentrations were measured by sampling the same air stream into the inlet of a GC-FID. Upon VOC addition, apparent ozone absorbances were observed to reach steady values within the initial 2–4 min with both the Hopcalite and MnO₂-based scrubbers. With the heated graphite scrubber, there was a rapid increase in apparent ozone upon addition, followed by a decay to steady values after 3 min. Average apparent ozone concentrations were obtained after 5 min of exposure and plotted

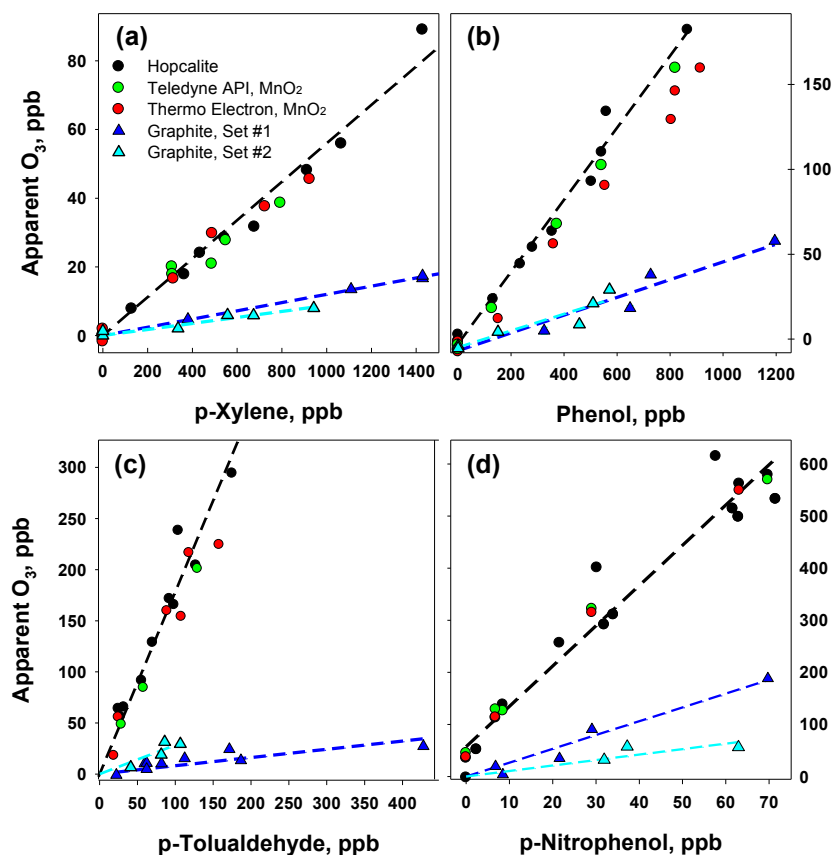


Figure 7. Apparent ozone vs. VOC concentration in dry, ozone-free air for different scrubber types and four different VOCs of varying absorption cross section at 253.7 nm. Data from two different sets of graphite tubes are shown (Set #1 and Set #2). Slopes are given in Table 2.

vs. VOC concentrations measured with the GC-FID (Fig. 7). There were no signs of surface saturation effects, as indicated by the linearity of the apparent ozone with VOC concentration plots. For all the compounds tested, the heated graphite scrubbers showed less apparent ozone. The slopes of the plots in Fig. 7 are given in Table 2. In all cases, the slopes were a factor of 2.5 to 20 less for the graphite scrubber than for Hopcalite or the MnO₂ scrubbers, indicating greatly reduced VOC uptake by the graphite. Data from two sets of graphite tubes (four tubes in parallel) gave identical results for both *p*-xylene and phenol; however, both *p*-tolualdehyde and *o*-nitrophenol exhibited slightly different apparent ozone values from these two different sets of graphite tubes. Responses for three other sets of graphite tubes were also tested against the Hopcalite scrubber and gave absorbances within the range of those shown in the figure. It remains unclear why different tube sets show slightly different behavior, but, again, it likely lies in the degree of graphite surface oxidation.

In dry air both Hopcalite and MnO₂ scrubbers exhibited similar responses for all the compounds tested. If the scrubbers remove 100 % of the VOC compound, then the slope of

these plots should be the inverse of the selectivity ratio reported in Table 1:

$$\frac{1}{S} = \text{Slope} = \frac{\sigma_{\text{VOC}-254 \text{ nm}}}{\sigma_{\text{O}_3-254 \text{ nm}}} \quad (\text{in ppb O}_3/\text{ppb VOC}). \quad (2)$$

There is good agreement in the theoretical slope and that observed for *p*-xylene (see Table 2), suggesting both Hopcalite and MnO₂-based scrubbers effectively scavenge all of the *p*-xylene in dry air. However, the slopes for phenol, *p*-tolualdehyde, and *o*-nitrophenol were all significantly higher by factors of 1.4, 3.3, and 4.1, respectively, than those computed from previously reported absorption cross sections. As this would require > 100 % removal by the scrubber, this can only be explained either by errors in the previously reported VOC cross sections or by an underestimation in the VOC concentrations via the GC technique. Since the error tends to decrease with volatility, the latter is more likely as it becomes more difficult to quantitatively desorb the VOC from the Tenax pre-concentration trap used in the GC. Furthermore, if our *o*-nitrophenol concentrations were correct, this suggests a 253.7 nm absorption cross section of nearly $9 \times 10^{-17} \text{ cm}^2 \text{ molecule}^{-1}$, which seems inexplicably large.

Table 2. Summary of results from tests of VOC interferences in dry air.

Volatile organic compound	Scrubber	Slope, ppb O ₃ /ppb VOC	S ^a , ppb VOC/ppb O ₃	S, previous results
<i>p</i> -Xylene	2B Hopcalite	0.056 ± 0.004	17.9	
	Thermo Electron (MnO ₂)	0.051 ± 0.003	19.6	
	Teledyne API (MnO ₂)	0.046 ± 0.005	21.7	
	Heated graphite	0.012 ± 0.001	83.3	
Phenol	2B Hopcalite	0.21 ± 0.01	4.76	7.7–14.3 ^b
	Thermo Electron (MnO ₂)	0.18 ± 0.01	5.56	
	Teledyne API (MnO ₂)	0.20 ± 0.01	5.00	
	Heated graphite	0.051 ± 0.004	19.6	
<i>p</i> -Tolualdehyde	2B Hopcalite	1.71 ± 0.25	0.58	0.0–2.0 ^c
	Thermo Electron (MnO ₂)	1.57 ± 0.43	0.63	
	Teledyne API (MnO ₂)	1.54 ± 0.10	0.65	1.25 ^c
	Heated graphite	0.08 ± 0.02	12.5	
		0.28 ± 0.06 ^d	3.6	
<i>o</i> -Nitrophenol	2B Hopcalite	7.7 ± 0.5	0.13	0.55–0.91 ^c
	Thermo Electron (MnO ₂)	8.0 ± 0.3	0.13	
	Teledyne API (MnO ₂)	7.4 ± 0.3	0.14	0.45 ^c
	Heated graphite	1.1 ± 0.3	0.91	
		2.7 ± 0.2 ^d	0.37	

^a $S = 1/\text{slope}$, measured selectivity ratio. ^b Zdanevitch (2002). ^c Spicer et al. (2010). ^d Results from two different sets of graphite tubes.

We did not pursue a more accurate GC-FID VOC quantitation, as the heated graphite scrubber can still be assessed on a relative basis to the conventional scrubbers from the ratios of the slopes in Fig. 7. Assuming that the packed-bed Hopcalite scrubber exhibits the theoretical selectivity factor based on absorption cross sections for each VOC tested (reported in Table 1), selectivity ratios of 83, 28, ≥ 12 , and ≥ 1.5 ppb VOC/ppb O₃ were estimated for *p*-xylene, phenol, *p*-tolualdehyde, and *o*-nitrophenol, respectively, for the heated graphite scrubber. In other words, it would require a *p*-xylene concentration of 83 ppb to produce a signal of 1 ppb O₃ in an analyzer using a heated graphite scrubber compared to a concentration of 20 ppb for the Hopcalite or MnO₂ scrubbers.

We observed less than a 10 % difference between the response ratios obtained with the Hopcalite and the two MnO₂ thin-film screen scrubbers for both *p*-tolualdehyde and *o*-nitrophenol in dry air. Spicer et al. (2010) report values of 0.8 and 0.0 to 0.5 ppb O₃/ppb *p*-tolualdehyde in dry air when using the MnO₂ and Hopcalite scrubbers, respectively, which is a difference of ≥ 30 %. They also report values of 2.2 and 1.1 to 1.8 ppb O₃/ppb *o*-nitrophenol for the MnO₂ and Hopcalite scrubbers. This leads to differences ranging from 20 % to a factor of 2, contrary to that observed in the current study. However, concentration levels of interfering VOCs were quite low in the Spicer et al. (2010) study, ranging from 7.6 to 14 ppb, and their measured apparent ozone mixing ratios were <15 ppb. At these levels, small signal drifts,

or the typical precision of ± 1 to 2 ppb in the ozone analyzers, impart significant uncertainty in the measured response ratio. It should be noted that the value of 0.8 ppb O₃/ppb *p*-tolualdehyde reported in Spicer et al. (2010) for the MnO₂ scrubber is also above the maximum theoretical response based on the reported absorption cross sections by a factor of 1.7 ($1/S = 0.48$, Table 1).

Zdanevitch (2002) reported a higher response for phenol and other VOCs studied with ozone present and suggested that photochemical production of stronger-absorbing compounds within the optical cell may be responsible. Our experiments with *p*-tolualdehyde and *p*-xylene failed to show such evidence for photochemical behavior. Absorbances recorded with both ozone and VOCs present were equivalent to the sum of the absorbances when these components were measured individually within the precision of the analyzer. This supports calculations that suggest negligible photochemistry can occur due to the low photon flux and short residence time in the 2B Technologies Model 202.

VOC interferences in humid air

Even at low humidity levels, water vapor is adsorbed to some extent by most of the conventional solid-phase scrubbers. This changes the surface characteristics of the solid phase, which, in turn, can alter the adsorption and desorption of other compounds. This is also dependent upon the properties of the species of interest – especially the particular com-

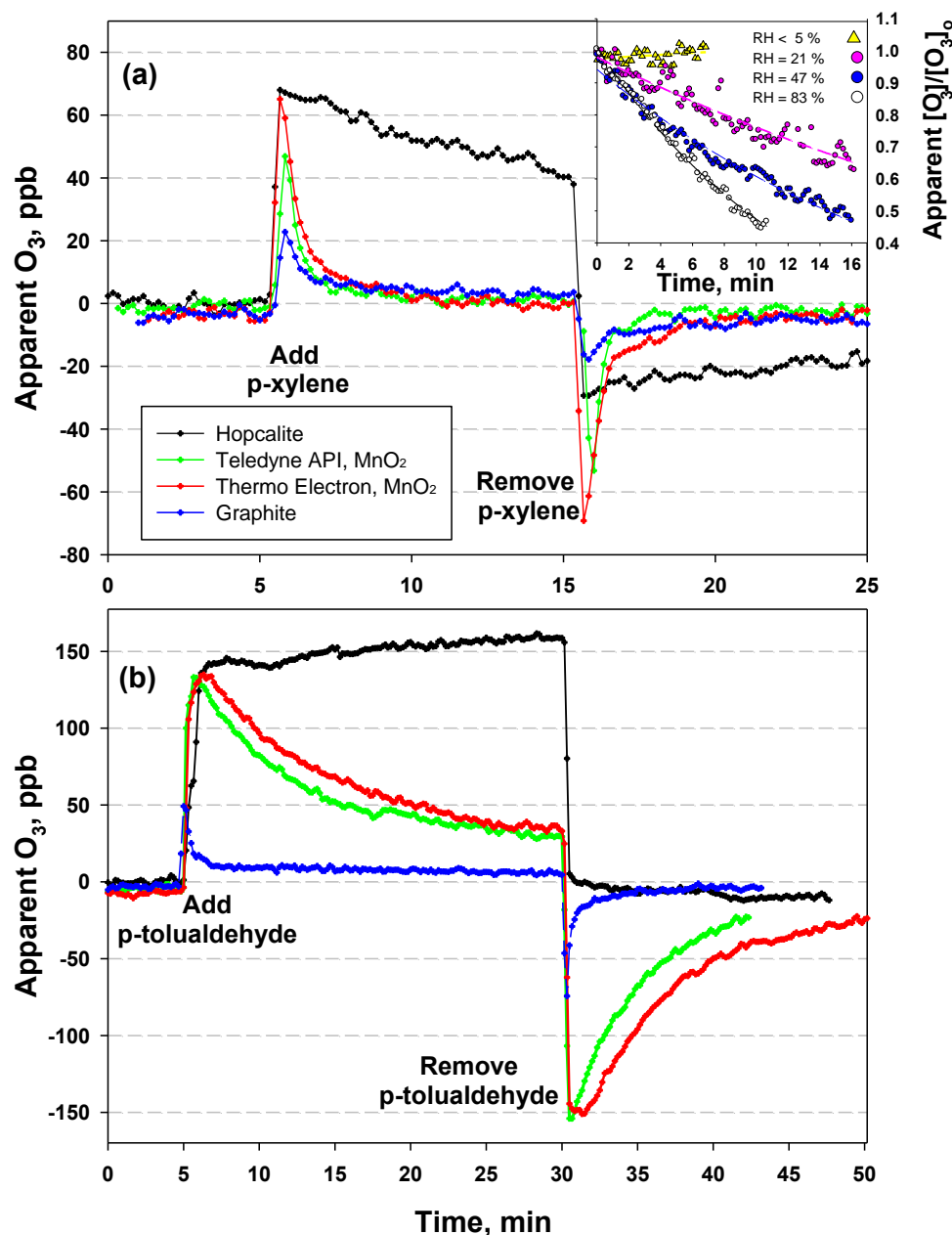


Figure 8. (a) Plot of the temporal behavior of the apparent ozone at 38 % RH as 1.2 ppm of *p*-xylene is added ($t = 5$ min) and then removed ($t = 15$ min) from ozone-free air for various scrubbers. Inset: temporal decay of the fractional apparent ozone ($[O_3]_0 =$ initial concentration) as a function of relative humidity upon addition of ~ 1.3 ppm of *p*-xylene to a Model 202 analyzer equipped with a packed-bed Hopcalite scrubber. (b) Temporal behavior of the apparent ozone at 75 % RH as ~ 90 ppb of *p*-tolualdehyde was added ($t = 5$ min) and then removed ($t = 30$ min) for various scrubbers.

pound's volatility. For the most volatile compound studied, *p*-xylene, even low levels of humidity caused the observed interference (apparent ozone) to decrease over time. Figure 8a shows the temporal behavior of the apparent ozone absorption upon addition of ~ 1 ppm of *p*-xylene in moderately humid ozone-free air with an analyzer equipped with a conventional packed-bed Hopcalite scrubber and Nafion.

There is an initial spike in the signal that then decays over time. The inset of Fig. 8a shows how this decay varied as a function of RH. In each case, *p*-xylene was added to generate an apparent ozone signal of ~ 80 ppb in dry air. The humidity was then changed within 20 seconds, and the absorbance decay was recorded. The apparent ozone decay was faster at

higher humidity, suggesting that the presence of water causes less *p*-xylene to be retained in the scrubber.

However, even at these higher water vapor concentrations, the scrubber still accumulated *p*-xylene. This is apparent upon turning off the *p*-xylene source, as a large negative absorbance was then observed (Fig. 8a). *p*-Xylene was now slowly desorbing from the scrubber material, thus absorbing more light during the I_0 measurement relative to I . This slow emission was also humidity dependent – becoming faster at higher relative humidity (data not shown). Scrubbers from the Thermo Electron and Teledyne API instruments show similar behavior, except that the time response is much faster (< 2 min, Fig. 8a), presumably due to the lower surface area of scrubber material. In fact, these scrubbers were observed to pass *p*-xylene nearly quantitatively, similar to the graphite scrubber after about 5 min as long as RH > 10%. These scrubbers also showed rapid release of the *p*-xylene once the VOC exposure was discontinued. However, the equilibration is rapid enough that, even at low humidity, the effect of xylenes on hourly averaged ambient ozone measurements is likely negligible with these low surface area scrubbers.

VOC responses with the heated graphite scrubber tend to be relatively insensitive to changes in relative humidity. Figure 9 shows a 1 ppm *p*-xylene addition to an ozone analyzer initially equipped with a Hopcalite scrubber at low RH (9%), giving an apparent O₃ concentration of 67 ppb. The Hopcalite was then exchanged for a heated graphite scrubber, and the relative humidity varied over the following 95 min where there is little to no RH-driven change in the observed absorbance. A plot of the averaged signal versus relative humidity yields a slope of 0.018 ppb apparent O₃/% RH, where a humidity change from 20 to 80% only alters the apparent ozone signal from 1 ppm of *p*-xylene by +1 ppb.

As the VOC becomes less volatile, the advantages of the heated graphite scrubber become more significant. Experiments with *p*-tolualdehyde indicated that a small amount of humidity (RH = 22%) did not alter the behavior from that observed in dry air for any of the various scrubbers. However, as RH increased to 75%, the coated MnO₂ screen scrubbers showed a large increase, followed by a slow decay over 20–30 min (Fig. 8b) – a behavior akin to the packed-bed Hopcalite–*p*-xylene exposure discussed previously. These scrubbers also exhibited a larger negative absorbance when the *p*-tolualdehyde flow was removed, indicating release of adsorbed *p*-tolualdehyde post-exposure, similar to the Hopcalite–*p*-xylene temporal profiles. For phenol, the selectivity for both the Hopcalite and MnO₂ scrubbers remained constant regardless of humidity (data not shown). Even at RH = 75%, the Hopcalite and MnO₂ scrubbers behaved similar to dry air, quantitatively removing phenol and showing no decay in the apparent O₃ absorbance over at least 10 min. We did not examine the behavior of *o*-nitrophenol with humidity, but presume it would be similar to that of phenol.

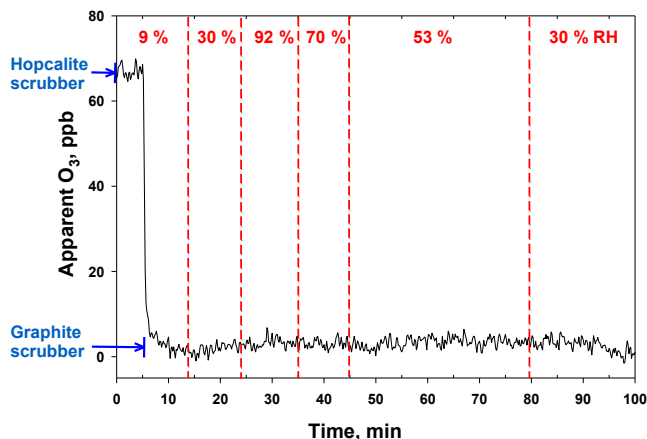


Figure 9. Apparent ozone observed upon addition of ~1.3 ppm of *p*-xylene to ozone-free air. Initially, the ozone analyzer was equipped with the standard Hopcalite scrubber (apparent O₃ concentration = 67 ppb). The Hopcalite was replaced with the heated graphite scrubber at time = 5 min. Over the next 95 min, the relative humidity of the air was varied as designated by the red vertical dashed lines.

Although the conventional MnO₂ scrubbers with low surface area appear to be compatible with the more volatile aromatics like xylene, their propensity to have uptake and re-emission of less volatile compounds dependent upon humidity levels is problematic in estimating ozone monitor biases. The selectivity ratio described above is now a function of humidity which varies in time. The wide variety of different atmospheric VOCs and their varying properties suggest that it will be nearly impossible to quantitatively model or estimate whether these scrubbers are consuming or releasing compounds, i.e., whether ozone monitors are biased negatively or positively. For example, Spicer et al. (2010) reported a decrease in the percent response ratio for the MnO₂ scrubber from 0.8 to 0.1 ppb *p*-tolualdehyde/ppb O₃ going from dry to humid air. This lowering of the *p*-tolualdehyde absorbance with RH was also observed in this study but was dependent upon exposure time such that a single selectivity ratio cannot be used. In contrast to the conventional solid-phase scrubbers, VOC interferences observed with the heated graphite scrubber are virtually insensitive to humidity changes for all the compounds studied. Although the graphite scrubber does retain a small fraction of the VOCs, the lack of a humidity dependence makes potential ozone monitor biases easier to predict.

4 Conclusions

A new solid-phase scrubber based on graphite for use in conventional ozone photometers was investigated and found to effectively remove ozone, while offering significant advantages over current ozone scrubbers with regard to species

that typically interfere in ozone measurements. When heated to 100–130 °C, the graphite scrubber quantitatively removed ozone up to 500 ppb – well above the concentration levels required for most ambient or indoor monitoring studies. After 2 weeks of ambient measurements in a single-beam instrument, slow oxidation of the graphite surface reduced its ability to completely remove ozone when operated at the lower end of the temperature range studied (≤ 100 °C). However, when operated at 130 °C, no loss of ozone removal efficiency was observed up to exposures of 30 ppm h over 38 days, and agreement with a conventional FEM analyzer was excellent throughout the time period. The higher temperature likely facilitates removal of lower-reactivity oxidized species from the graphite surface either by enhancing desorption or the reaction rate with ozone. Therefore, long-term measurements require continuous operation near the maximum of 130 °C or periodic regeneration of the scrubber by heating it to 150 °C for 20–30 min. These conditions appear to be valid for both single-beam and dual-beam monitors.

The major advantage of the heated graphite scrubber is its ability to pass many of the known atmospheric interferences that plague conventional solid-phase ozone scrubbers. Elimination of small biases of a few ppb of ozone can be critical in marginal compliance situations where ambient ozone is near the NAAQS. Water effects on ozone measurements (through refractive index changes in the optical cell) were virtually eliminated by use of the graphite scrubber, thereby eliminating the need for humidity equilibration using Nafion. Gas-phase mercury interference was $\leq 3\%$ of a packed-bed Hopcalite scrubber and at least a factor of 2 better than other conventional MnO₂ coated-screen scrubbers. The graphite scrubber was also observed to consistently exhibit smaller interferences in dry air for a series of substituted aromatic compounds ranging in volatility and extinction coefficient. The apparent ozone absorptions measured with the graphite scrubber were typically a factor of 2.5 to 20 smaller than those with the conventional Hopcalite or MnO₂ scrubbers. Our results suggest that to generate an absorbance equivalent to 1 ppb of ozone would necessitate concentrations of 83 ppb of *p*-xylene, 28 ppb of phenol, ≥ 12 ppb of *p*-tolualdehyde, ≥ 1.5 ppb of *o*-nitrophenol, or ≥ 25 ppt of mercury vapor. These are nearly 3 or more times greater than typical ambient concentrations for any of these species (Table 1).

The small VOC interference observed with the graphite scrubber was also insensitive to humidity level. Although the conventional commercial solid-phase scrubbers tended to remove all of the aromatic VOCs studied in dry air, these scrubbers tended to show less interferences at higher humidity levels (i.e., less aromatic compounds retained in the scrubber). This lowering of the interference was tied to the particular VOC's intrinsic volatility and the surface area of the solid-phase scrubber. Low-volatility compounds (such as phenol) were retained regardless of humidity level, whereas compounds with higher volatility (*p*-xylene) were nearly quantitatively passed by the scrubbers using coated screens

with low surface area. For compounds that were intermediate in volatility, such as *p*-tolualdehyde, the conventional commercial scrubbers quantitatively removed the VOC at low humidity ($< 40\%$ RH), but the coated-screen scrubbers showed a slow equilibration at high water vapor concentrations ($> 70\%$ RH, $t_{\text{equil}} \sim 30$ min.). These also released *p*-tolualdehyde upon ending exposure to the compound. These results strongly suggest that these scrubbers tend to accumulate VOCs under drier conditions (creating a positive bias in ozone analyzers) and then subsequently rerelease them as humidity is increased (creating the possibility of a negative bias). This complex behavior involving humidity and volatility is avoided by use of the heated graphite scrubber.

Although more work is needed to determine whether the graphite scrubber can replace conventional solid-phase scrubbers for long-term compliance monitoring, both the lab and field studies presented here suggest that the heated graphite scrubber has the potential to provide more accurate ozone concentration measurements by reducing conventional photometer susceptibility to many common interferences. The operating characteristics (flow, pressure, etc.) of the heated graphite scrubber are also compatible with most conventional ozone monitors. Reducing interferences in ozone measurements is especially important for ozone monitoring in highly polluted regions or in applications where high levels of VOCs or mercury exist, such as in smog chamber experiments, indoor environments, or near areas of mercury contamination. It may also prove to be important in areas of marginal noncompliance with ambient ozone standards.

Data availability. Experimental data presented here are available upon request to the authors (andrewt@twobtech.com).

Competing interests. All authors are employees of 2B Technologies, Inc., which produces commercial UV-absorbance ozone monitors including the instruments used in this work.

Acknowledgements. The authors would like to acknowledge John Ortega at the National Center for Atmospheric Research for assistance with GC-FID measurements. We would also like to thank Will Ollison for his advice and critique of this manuscript.

Edited by: T. F. Hanisco

Reviewed by: two anonymous referees

References

- Avnery, S., Mauzerall, D. L., Liu, J., and Horowitz, L. W.: Global crop yield reductions due to surface ozone exposure: 1. Year 2000 crop production losses and economic damage, *Atmos. Environ.*, 45, 2284–2296, 2011.

- Bernardo-Bricker, A., Farmer, C. Milne, P., Riemer, D., Zika, R., and Stoneking, C.: Validation of speciated nonmethane hydrocarbon compound data collected during the 1992 Atlanta Intensive as part of the Southern Oxidants Study, *J. Air Waste Manage.*, 45, 591–603, 1995.
- Birks, J. W., Williford, C. J., and Andersen, P. C.: Use of a Broad Band UV Light Source for Reducing the Mercury Interference in Ozone Measurements, U.S. Patent Application US 2009/0302230 A1, US Patent and Trademark Office, Washington, D.C., USA, 2009.
- Birks, J. W., Andersen, P. C., and Williford, C. J.: Ozone monitor with gas-phase scrubber, U.S. Patent US 8,395,776 B2, US Patent and Trademark Office, Washington, D.C., USA, 2013.
- Birks, J. W., Turnipseed, A. A., Andersen, P. C., and Williford, C. J.: Heated Graphite Scrubber to Reduce Interferences in Ozone Monitors, U.S. Patent US 2016/0025696 A1, US Patent and Trademark Office, Washington, D.C., USA, 2016.
- Burkholder, J. B., Sander, S. P., Abbatt, J., Barker, J. R., Huie, R. E., Kolb, C. E., Kurylo, M. J., Orkin, V. L., Wilmouth, D. M., and Wine, P. H.: Chemical Kinetics and Photochemical Data for Use in Atmospheric Studies, Evaluation No. 18, JPL Publication 15-10, Jet Propulsion Laboratory, Pasadena, USA, 2015.
- Burnett, R. T., Brook, J. R., Yung, W. T., Dales, R. E., and Krewski, D.: Association between ozone and hospitalization for respiratory diseases in 16 Canadian cities, *Environ. Res.*, 72, 24–31, 1997.
- Carpi, A. and Chen, Y. F.: Gaseous elemental mercury as an indoor air pollutant, *Environ. Sci. Technol.*, 35, 4170–4173, 2001.
- Chameides, W. L. and Walker, J. C. G.: A photochemical theory of tropospheric ozone, *J. Geophys. Res.*, 78, 8751–8759, 1973.
- Davies, L.: Nitrobenzene, International Programme on Chemical Safety – Environmental Health Criteria 230, World Health Organization, Geneva, Switzerland, 2003.
- Delhomme, O., Morville, S., and Millet, M.: Seasonal and diurnal variations of atmospheric concentrations of phenols and nitrophenols measured in the Strasborg area, France, *Atmos. Pollut. Res.*, 1, 16–22, 2010.
- Denis, M. St., Song, X., Lu, J. Y., and Feng, X.: Atmospheric gaseous elemental mercury in downtown Toronto, *Atmos. Environ.*, 40, 4016–4024, 2006.
- Dumarey, R., Dams, R., and Hoste, J.: Comparison of the collection and desorption efficiency of activated charcoal, silver and gold for the determination of vapor-phase atmospheric mercury, *Anal. Chem.*, 57, 2638–2644, 1985.
- Dunlea, E. J., Herndon, S. C., Nelson, D. D., Volkamer, R. M., Lamb, B. K., Allwine, E. J., Grutter, M., Ramos Villegas, C. R., Marquez, C., Blanco, S., Cardenas, B., Kolb, C. E., Molina, L. T., and Molina, M. J.: Technical note: Evaluation of standard ultraviolet absorption ozone monitors in a polluted urban environment, *Atmos. Chem. Phys.*, 6, 3163–3180, <https://doi.org/10.5194/acp-6-3163-2006>, 2006.
- Eiguren-Fernandez, A., Miguel, A. H., Foines, J. R., Thurairatnam, S., and Avol, E. L.: Seasonal and spatial variation of polycyclic aromatic hydrocarbons in vapor-phase and PM_{2.5} in Southern California urban and rural communities, *Aerosol Sci. Tech.*, 38, 447–455, 2004.
- Ellis, W. D. and Tometz, P. V.: Room-temperature catalytic decomposition of ozone, *Atmos. Environ.*, 6, 707–714, 1972.
- Emberson, L., Ashmore, M., and Murray, F.: Air Pollution Impacts on Crops and Forests. A Global Assessment, Imperial College Press, London, UK, 2003.
- Emberson, L. D., B ker, P., Ashmore, M. R., Mills, G., Jackson, L. S., Agrawal, M., Atikuzzaman, M. D., Cinderby, S., Engardt, M., Jamir, C., Kobayashi, K., Oanh, N. T. K., Quadir, Q. F., and Wahid, A.: A comparison of North American and Asian exposure–response data for ozone effects on crop yields, *Atmos. Environ.*, 43, 1945–1953, 2009.
- Entegris: Properties and characteristics of graphite, available at: <https://www.entegris.com/content/dam/web/resources/manuals-and-guides/manual-properties-and-characteristics-of-graphite-109441.pdf> (last access: 12 June 2017), 2015.
- Fang, F., Wang, Q., and Li, J.: Urban environmental mercury in Changchun, a metropolitan city in Northeastern China: Source, cycle, and fate, *Sci. Total Environ.*, 330, 159–170, 2004.
- Finlayson-Pitts, B. J. and Pitts, J. N.: Chemistry of the Upper and Lower Atmosphere: Theory, Experiments and Applications, Academic Press, San Diego, USA, 2000.
- Garetano, G., Gochfeld, M., and Stern, A. H.: Comparison of indoor mercury vapor in common areas of residential buildings with outdoor levels in a community where mercury is used for cultural purposes, *Environ. Health Perspect.*, 114, 59–62, 2006.
- Greenberg, J. P., Lee, B., Helmig, D., and Zimmerman, P. R.: Fully automated gas chromatograph-flame ionization detector system for the in situ determination of atmospheric non-methane hydrocarbons at low parts per trillion concentration, *J. Chrom. A.*, 676, 389–398, 1994.
- Griffin, R. J., Cocker, D. R., Flagan, R. C., and Seinfeld, J. H.: Organic aerosol formation from the oxidation of biogenic hydrocarbons, *J. Geophys. Res.*, 104, 3555–3567, 1999.
- Grosjean, D. and Harrison, J.: Response of chemiluminescent NO_x analyzers and ultraviolet ozone analyzers to organic air pollutants, *Environ. Sci. Technol.*, 19, 862–865, 1985.
- Haagen-Smit, A. J. and Fox, M. M.: Photochemical ozone formation with hydrocarbons and automobile exhaust, *J. Air Pollut. Control Assoc.*, 4, 105–108, 1954.
- Hennig, G. R.: Anisotropic reactivities of graphite – I. Reactions of ozone and graphite, *Carbon*, 3, 107–114, 1965.
- Huntzicker, J. A. and Johnson, R. L.: Investigations of an ambient interference in the measurement of ozone by ultraviolet photometry, *Environ. Sci. Technol.*, 13, 1414–1416, 1979.
- Keller-Rudek, H., Moortgat, G. K., Sander, R., and S rensen, R.: The MPI-Mainz UV/VIS Spectral Atlas of Gaseous Molecules of Atmospheric Interest, *Earth Syst. Sci. Data*, 5, 365–373, <https://doi.org/10.5194/essd-5-365-2013>, 2013.
- Kim, K. H. and Kim, M. Y.: A decadal shift in total gaseous mercury concentration levels in Seoul, Korea: changes between the late 1980s and the late 1990s, *Atmos. Environ.*, 36, 663–675, 2002.
- Kleindienst, T. E., Hudgens, E. E., Smith, D. F., McElroy, F. F., and Bufalini, J. J.: Comparison of chemiluminescence and ultraviolet ozone monitor responses in the presence of humidity and photochemical pollutants, *J. Air Waste Manage.*, 43, 213–222, 1993.
- Lee, A., Goldstein, A. H., Keywood, M. D., Gao, S., Varutbangkul, V., Bahreini, R., Ng, N. L., Flagan, R. C., and Seinfeld, J. H.: Gas-phase products and secondary aerosol yields from the ozonolysis of ten different terpenes, *J. Geophys. Res.*, 111, D07302, <https://doi.org/10.1029/2006JD007050>, 2006.

- Lee, P. and Davidson, J.: Evaluation of activated carbon filters for removal of ozone at the ppb level, *J. Am. Ind. Hyg.*, 60, 589–600, 1999.
- Leston, A. R., Ollison, W. M., Spicer, C. W., and Satola, J.: Potential interference bias in ozone standard compliance monitoring, *J. Air Waste Manage.*, 55, 1464–1472, <https://doi.org/10.1080/10473289.2005.10464749>, 2005.
- Li, Y., Lee, S.-R., and Wu, C.-Y.: UV-absorption-based measurements of ozone and mercury: an investigation on their mutual interferences, *Aerosol Air Quality Res.*, 6, 418–429, 2006.
- Liu, S., Nadim, F., Perkins, C., Carley, R. J., Hoag, G. E., Lin, Y., and Chen, L.: Atmospheric mercury monitoring survey in Beijing, China, *Chemosphere*, 48, 97–107, 2002.
- Mahmoud, F. M., Kang, D., and Aneja, V. P.: Volatile organic compounds in some urban locations in the United States, *Chemosphere*, 47, 863–882, 2002.
- McCarthy, J. E. and Lattanzio, R. K.: Ozone Air Quality Standards: EPA's 2015 Revision, Congressional Research Reports Publication #R43092, available at: <https://fas.org/sgp/crs/misc/R43092.pdf> (last access: 12 June 2017), 2016.
- Meyer, C. P., Elsworth, C. M., and Galbally, I. E.: Water vapor interference in the measurement of ozone in ambient air by ultraviolet absorption, *Rev. Sci. Instrum.*, 62, 223–228, 1991.
- Obrist, D., Hallar, A. G., McCubbin, I., Stephens, B. B., and Rahn, T.: Atmospheric mercury concentrations at Storm Peak Laboratory in the Rocky Mountains: Evidence for long-range transport from Asia, boundary layer contributions, and plant mercury uptake, *Atmos. Environ.*, 42, 7579–7589, 2008.
- Ollison, W. M., Crow, W., and Spicer, C. W.: Field testing of new technology ambient air ozone monitors, *J. Air Waste Manage.*, 63, 855–863, <https://doi.org/10.1080/10962247.2013.796898>, 2013.
- Parrish, D. D. and Fehsenfeld, F. C.: Methods for gas-phase measurements of ozone, ozone precursors and aerosol precursors, *Atmos. Environ.* 34, 1921–1957, 2000.
- Razumovskii, S. D., Gorshenev, V. N., Kovarskii, A. L., Kuznetsov, A. M., and Shchegolikhin, A. N.: Carbon nanostructure reactivity: Reactions of graphite powders with ozone, *Fuller. Nanotub. Car. N.*, 15, 53–63, 2007.
- Ryerson, T. B., Buhr, M. P., Frost, G. J., Goldan, P. D., Holloway, J. S., Hubler, G., Jobson, B. T., Kuster, W. C., McKeen, S. A., Parrish, D. D., Roberts, J. M., Sueper, D. T., Trainer, M., Williams, J., and Fehsenfeld, F. C.: Emissions lifetimes and ozone formation in power plant plumes, *J. Geophys. Res.*, 103, 22569–22583, 1998.
- Saathoff, H., Kamm, S., Möhler, O., Naumann, K.-H., and Schurath, U.: Kinetics and Mechanism of the Heterogeneous Interaction of Ozone with Soot Aerosol, *J. Aerosol Sci.*, 29, S889–S890, 1998.
- Seila, R. L., Lonneman, W. A., and Meeks, S. A.: Determination of C2 to C12 ambient air hydrocarbons in 39 U.S. cities from 1984 through 1986, EPA report /600/S3-89/058, Springfield, USA, 1989.
- Shields, H. C., Weschler, C. W., and Naik, D.: Ozone removal by charcoal filters after continuous extensive use (5 to 8 years), Proceedings of the 8th International Conference on Indoor Air Quality and Climate, Indoor Air 99, 8–13 August 1999, Edinburgh, UK, Vol. 4, 49–54, 1999.
- Smith, D. M. and Chughtai, A. R.: Reaction Kinetics of Ozone at Low Concentrations with n-Hexane Soot, *J. Geophys. Res.*, 101, 19607–19620, 1996.
- Spicer, C. W., Joseph, D. W., and Ollison, W. M.: A re-examination of ambient air ozone monitor interferences, *J. Air Waste Manage.*, 60, 1353–1364, <https://doi.org/10.3155/1047-3289.60.11.1353>, 2010.
- Stephens, S. L., Birks, J. W., and Calvert, J. G.: Ozone as a Sink for Atmospheric Carbon Aerosols Today and Following Nuclear War, *Aerosol Sci. Technol.*, 10, 326–331, 1989.
- Tracz, A., Wegner, G., and Rabe, J. P.: Scanning tunneling microscopy study of graphite oxidation in ozone-air mixtures, *Langmuir*, 19, 6807–6812, 2003.
- U.S.-EPA: Laboratory Study to Explore Potential Interferences to Air Quality Monitors, EPA-454/C-00-002, Office of Air Quality Planning and Standards: Research Triangle Park, NC, USA, 1999.
- U.S.-EPA: Health Effects of Ozone in the General Population, available at: <https://www.epa.gov/ozone-pollution-and-your-patients-health/health-effects-ozone-general-population>, last access: October 2016.
- Weisel, C. P., Cody, R. P., and Liou, P. J.: Relationship between summertime ambient ozone levels and emergency department visits for asthma in central New Jersey (suppl. 2), *Environ. Health Perspect.*, 103, 97–102, 1995.
- Weiss-Penzias, P., Jaffe, D. A., McClintick, A., Prestbo, E., and Landis, M. S.: Gaseous elemental mercury in the marine boundary layer: Evidence for rapid removal in anthropogenic pollution, *Environ. Sci. Technol.*, 37, 3755–3763, 2003.
- White, M. C., Etzel, R. A., Wilcox, W. D., and Lloyd, C.: Exacerbations of childhood asthma and ozone pollution in Atlanta, *Environ. Res.*, 65, 56–68, 1994.
- Wilson, K. L. and Birks, J. W.: Mechanism and elimination of a water vapor interference in the measurement of ozone by UV absorbance, *Environ. Sci. Technol.*, 40, 6361–6367, 2006.
- Zdanevitch, I.: Study of Ozone Measurement Interferences: Final Report, DRC-02-39246-AIRE-673-v2-Izd; Institut National de L'Environnement Industriel et des Risques (INERIS), Verneuil-en-Halatte, France, 2002.